

metric TDHF calculations with no free parameters are able to reproduce quantitatively the essential features observed in the $^{208}\text{Pb} + ^{208}\text{Pb}$ reaction. Altogether, with the successful test of the theory in Kr-induced reactions⁸ this calculation in a mass region which has so far only merely been explored confirms that the TDHF theory provides us with a very viable and a promising microscopic tool for the description of heavy-ion collisional phenomena.

Thanks are due to P. Bonche for his very critical reading of the manuscript. This study owes a lot to the cooperation of B. S. Nilsson. Discussions with him, J. P. Bondorf, J. Randrup, R. Schaeffer, and G. Wolshin are gratefully acknowledged. Financial grants from the Danish Research Council and Commemorative Association of the Japan world exposition are also acknowledged. The author also wishes to acknowledge the hospitality of the Centre d'Etudes Nucléaires de Saclay, where the final phase of this work was carried out.

¹P. Bonche, S. E. Koonin, and J. W. Negele, *Phys. Rev. C* **13**, 1226 (1976).

²S. E. Koonin, K. T. R. Davies, V. Maruhn-Rezwani, H. Feldmeier, S. J. Krieger, and J. W. Negele, *Phys. Rev. C* **15**, 1359 (1977).

³P. Bonche, B. Grammaticos, and S. E. Koonin, *Phys. Rev. C* **17**, 1700 (1978).

⁴H. Flocard, S. E. Koonin, and M. S. Weiss, *Phys. Rev. C* **17**, 1682 (1978).

⁵A. K. Dhar and B. S. Nilsson, *Nucl. Phys.* **A315**, 445 (1979), and references therein.

⁶A. K. Dhar, B. S. Nilsson, and H. Jaqaman, Niels Bohr Institute Report No. NBI 78-31 (to be published).

⁷A. K. Dhar and B. S. Nilsson, *Phys. Lett.* **77B**, 50 (1978).

⁸K. T. R. Davies, V. Maruhn-Rezwani, S. E. Koonin, and J. W. Negele, *Phys. Rev. Lett.* **41**, 632 (1978).

⁹H. Sann, A. Olmi, Y. Civelekoglu, D. Pelte, U. Lynen, H. Stelzer, A. Gobbi, Y. Eyal, W. Kohl, R. Renfordt, I. Rode, G. Rudolf, D. Schwalm, and R. Bock, in *Proceedings of the Topical Conference on Heavy Ion Collisions, Fall Creek Falls State Park, Tennessee, 1977*, CONF-770602 (National Technical Information Service, Springfield, Va., 1977), p. 281.

¹⁰U. Lynen, Y. Civelekoglu, A. Olmi, H. Sann, D. Pelte, R. Bock, A. Gobbi, and H. Stelzer, *Gesellschaft für Schwerionenforschung Annual Report 1977*, Report No. GSI-J-1-78, 1978 (unpublished), p. 55.

¹¹The charge radius has been computed using the proton rms radius of 0.8 fm.

¹²I also performed a TDHF calculation for $l = 400\hbar$ with the clutching density approximation. No noticeable change in the energy loss and final c.m. scattering angle was obtained. An unphysical feature of this approximation is the change in the total energy by about 20 MeV at the point of contact and separation of the two fragments.

¹³The ions are assumed to have moved along the Coulomb trajectory (appropriate for the specific L value) from $t = -\infty$ to a relatively large separation (28 fm) chosen at $t = 0$. My E/A value of 7.4 MeV/amu includes the Coulomb polarization effects as well.

¹⁴C. Dasso, T. Døssing, and H. C. Pauli, to be published, and private communication.

¹⁵K. T. R. Davies, A. Sierk, and J. R. Nix, *Phys. Rev. C* **13**, 2385 (1976).

Free-Free Transitions Following Six-Photon Ionization of Xenon Atoms

P. Agostini, F. Fabre, G. Mainfray, and G. Petite

Centre d'Etudes Nucléaires de Saclay, Service de Physique Atomique, 91190 Gif-sur-Yvette, France

and

N. K. Rahman

Laboratorio di Chimica Quantistica ed Energetica Molecolare del Consiglio Nazionale delle Ricerche, 56100 Pisa 35, Italy

(Received 29 January 1979)

The energy spectrum of electrons produced by multiphoton ionization of xenon atoms has been analyzed with a retarding potential technique. We have shown that the discrete absorption of photons above the six-photon ionization threshold was observable under specified conditions. A simple model based upon inverse bremsstrahlung gives a reasonable agreement with the experiments.

A recent aspect of the experiments on multiphoton ionization of atoms is the measurement of the electron energy spectrum. The principal reason

for observing the energy of the emitted electrons is to discover whether, at the intensities involved, the bound electron absorbs preponderantly the

minimum of photons necessary for the atom to be ionized or whether additional absorption of photons in the continuum is of significance. In this Letter we report the first measurement of the electron energy spectrum in which the above-mentioned effects have been detected.

Consider xenon atoms (ionization potential = 12.27 eV) and Nd⁺⁺⁺-glass laser ($\hbar\omega = 1.17$ eV). The eleven-photon ionization, to be measurable requires intensities of the order of 10^{13} W cm⁻² for a bandwidth-limited laser.¹ The absorption of a twelfth photon will result mainly in an increase of the emitted electron energy by $\hbar\omega$ as shown in Fig. 1(a).

The induced modifications of the electron energy spectrum can be concealed by another physical mechanism of acceleration of the free electrons due to the gradient of the electromagnetic field.² The resulting force can be shown to be conservative and is given by

$$f = (-e/2m\omega^2)\nabla(E^2), \quad (1)$$

where E is the electric field, ω is the light frequency, and e and m are the electron charge and mass. In the high-intensity limit the maximum energy the electron can gain depends only on the intensity and is given by

$$E_{\max}(\text{eV}) = 1.048 \times 10^{-13} I (\text{W cm}^{-2}) \quad (2)$$

for the fundamental frequency of a Nd⁺⁺⁺-glass laser.

Previous experiments concerned with electron

energy measurement in multiphoton ionization seem to have measured this acceleration,^{3,4} and no evidence of discrete photon absorption above threshold has been obtained. To reduce this acceleration, one can attempt to diminish the gradient and/or increase the frequency. At intensities of a few 10^{13} W cm⁻², formula (2) gives a maximum energy for the electrons of a few electron volts, which is somewhat larger than the energy of one photon (1.17 eV). Therefore one expects to observe a continuous energy distribution around a maximum given by formula (2). On the other hand, in the case of the second-harmonic frequency, the six-photon ionization of xenon requires intensities roughly 5 times lower and E_{\max} , as given by Eqs. (1) and (2), will be about 20 times smaller, i.e., 0.2–0.3 eV. Since the energy spreading due to the gradient acceleration is much smaller than the photon energy (2.34 eV), the lines corresponding to discrete photon absorption should be much more easily resolved.

The experimental arrangement was as follows: A single-mode, passively Q-switched Nd⁺⁺⁺-glass oscillator produced 12-ns, 5-mJ pulses. After suitable amplification, pulses of about 2 J were obtained. The beam diameter was reduced to 6 mm by a telescope and focused inside a vacuum chamber by a 70-mm-focal-length spherical lens. The second harmonic was generated, when necessary, by a potassium dihydrogen phosphate (KDP) crystal set after the telescope. The interaction chamber was filled with Xe at a pressure of about 5×10^{-5} Torr.

A double Netic and Co-Netic shielding box surrounded the region of the focus of the lens thus reducing the magnetic field to 5×10^{-2} G. The electrons created at the focus of the lens could diffuse in the field-free space inside the box. Some of them eventually left the box through a high-transparency (90%) mesh. In order to analyze the electrons' energy, a potential barrier was established by setting the box to some voltage V_R positive compared to a grounded second mesh (see Fig. 2). Those electrons with energies higher than the potential barrier were then accelerated to about 200 eV and detected by a separated-dynodes electron multiplier tube (EMT). The EMT, supplied with positive high voltage on the last dynode, had a gain of about 5×10^6 . The anode electron current was measured on a 7A22 Tektronix plug-in unit and displayed on a 7633 storage oscilloscope. The EMT signal, when plotted against the retarding voltage V_R , gives the integral energy distribution of the electrons

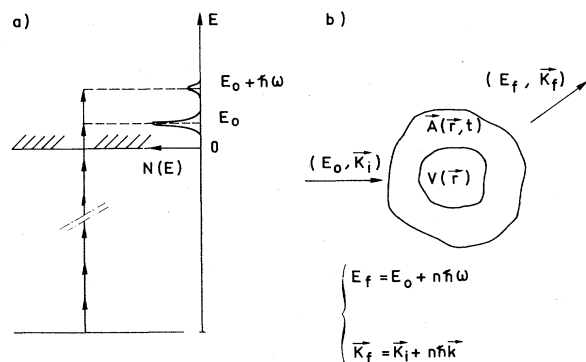


FIG. 1. (a) Schematic diagram of energy levels for multiphoton ionization at threshold and above, together with the energy spectrum of the emitted electrons. (b) Inelastic electron scattering by a scalar potential $V(\vec{r})$ in the presence of an electromagnetic field. E_0, K_i (E_f, K_f) are the initial (final) electrons' energy and momentum. ω is the frequency of the electromagnetic field.

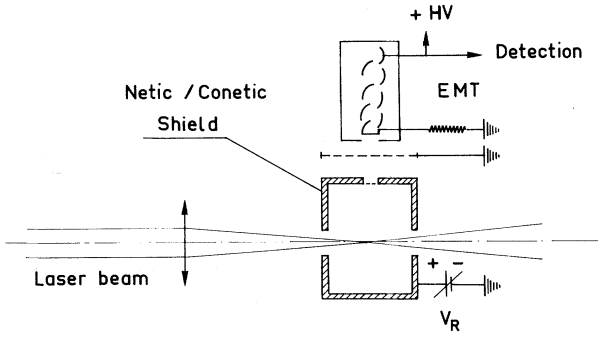


FIG. 2. Schematic of the experimental apparatus.

since it is proportional to $\int_0^\infty N(E) dE$, where $N(E)$ is the spectral density at the energy E . This integral distribution can be numerically differentiated in order to obtain $N(E)$.

The laser was linearly polarized and the direction of electron detection was parallel to the laser polarization in the case of the fundamental frequency and perpendicular in the case of the second harmonic.

The results of a typical measurement for the fundamental frequency are shown in Fig. 3. The intensity was about $4 \times 10^{13} \text{ W cm}^{-2}$ with a pulse duration of 12 ns. The electron energy spectrum does not show any evidence of a discrete structure.

This result is explained by the acquisition of energy due to the gradient of the electric field and serves to substantiate similar previous findings concerning the same mechanism.^{4, 5} The electron mean energy ($\approx 4 \text{ eV}$) is in good agreement with the value predicted by formula (2) for a laser intensity of $4 \times 10^{13} \text{ W cm}^{-2}$.

In the same figure appear the results obtained with the second harmonic of the same laser. The pulse duration was 10 ns and the peak intensity about $8 \times 10^{12} \text{ W/cm}^{-2}$.

Firstly, we note the peak at energy $E \approx 2 \text{ eV}$ which is very close to the energy of the electron emitted with six-photon ionization of Xe ($E_0 \approx 1.90 \text{ eV}$). It is evident from the figure that most of the electrons (90%) measured were found at this energy.

A secondary peak appears at $E \approx 4.5 \text{ eV}$ which is in very good agreement with the value $E_0 + \hbar\omega$, where $\hbar\omega = 2.34 \text{ eV}$. We therefore conclude that the seven-photon process including one free-free transition has been detected in this experiment.

Unfortunately there exists no reliable calculation for the multiphoton ionization of Xe, and

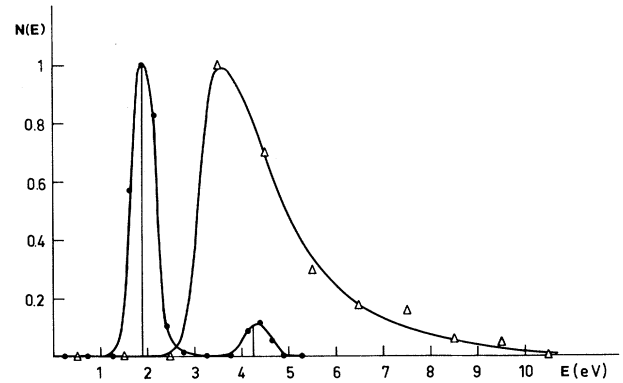


FIG. 3. Energy spectra of the emitted electrons for two photon energies: triangles, $\hbar\omega = 1.17 \text{ eV}$, $I = 4 \times 10^{13} \text{ W/cm}^{-2}$, $E_{\text{max}} = 4 \text{ eV}$; circles, $\hbar\omega = 2.34 \text{ eV}$, $I = 8 \times 10^{12} \text{ W/cm}^{-2}$, $E_{\text{max}} = 0.2 \text{ eV}$ (E_{max} is the maximum energy gained in the field gradient). The solid straight lines at 1.90 and 4.25 eV have heights proportional to the values of $(d\sigma^{(M)}/d\Omega)$ $(d\sigma^{(e1)}/d\Omega)^{-1}$ calculated from Eq. (3) using an intensity of $1.0 \times 10^{13} \text{ W/cm}^{-2}$. The solid curves have been hand drawn through the experimental points.

moreover, the question of the absorption of additional photons beyond the ionization threshold is only beginning to be investigated.⁵ For these reasons, we have preferred to model this additional absorption of photons in the following simplified manner: the electrons emitted by the N -photon ionization constitute a monoenergetic (E_0) collection of free electrons. These electrons can now absorb additional photons in the presence of the ion potential [inverse bremsstrahlung, see Fig. 1(b)]. The differential cross section for the M -photon inverse bremsstrahlung is given by⁶

$$\frac{d\sigma^{(M)}}{d\Omega} = \frac{K_f}{K_i} J_M^2 \left[\frac{e \vec{A}(\vec{K}_f - \vec{K}_i)}{-m\omega} \right] \frac{d\sigma^{(e1)}}{d\Omega}, \quad (3)$$

where \vec{A} is the vector potential, \vec{K}_i (\vec{K}_f) are the initial (final) electron momentum, J_M is the Bessel function of order M , and $d\sigma^{(e1)}/d\Omega$ is the elastic differential cross section of electron scattering in the potential. This formula has been experimentally qualitatively verified.⁷ Since we had no *a priori* knowledge of the angular distribution of the "initial" free electrons, we have utilized both an isotropic as well as a peaked function to average over the initial angular distribution, with similar results. The signal calculated from Eq. (3) using an intensity of $1.0 \times 10^{13} \text{ W/cm}^{-2}$ is shown as the two lines positioned at $E = 1.90$ and 4.25 eV . All the results (experimental and theoretical) have been normalized to 1 for the first peak. A

reasonable fit is obtained for intensity values from 8×10^{12} to 2×10^{13} W cm^{-2} , in good agreement with the experimental value $(8 \pm 2) \times 10^{12}$ W cm^{-2} . One should note that at this intensity, and for the second harmonic, formula (2) gives an energy gain in the gradient of the field of 0.25 eV which is compatible with the experimental width of the peaks of 0.5 eV and which, in any case, leaves the two peaks well resolved.

We are in the process of obtaining additional information regarding the electrons emitted in N -photon ionization. These include the measurement of angular distribution and the dependence on polarization. A comprehensive account will be published elsewhere.

We finally wish to remark that our measure-

ment has been the first to detect an additional photon absorption beyond the minimum number necessary for ionization of an atom.

¹L. A. Lompre, G. Mainfray, C. Manus, and J. Thebault, *Phys. Rev. A* **15**, 1604 (1977).

²T. W. B. Kibble, *Phys. Rev. A* **150**, 1060 (1966).

³E. A. Martin and L. Mandel, *Appl. Opt.* **15**, 2378 (1976).

⁴M. J. Hollis, *Opt. Commun.* **25**, 395 (1978).

⁵E. Karule, *J. Phys. B* **11**, 441 (1978).

⁶N. K. Rahman, *Phys. Rev. A* **10**, 440 (1974).

⁷A. Weingarsthofer, J. K. Holmes, G. Candle, E. Clarke, and H. Kruger, *Phys. Rev. Lett.* **39**, 269 (1977).

Measurement of Differential Cross Sections for the Elastic Scattering of Positrons by Argon Atoms

P. G. Coleman and J. D. McNutt

Department of Physics, The University of Texas at Arlington, Arlington, Texas 76019

(Received 14 December 1978)

Direct measurements of differential scattering cross sections for positron-gas-atom collisions are reported. The apparatus used exploits the time-of-flight technique. Results for positrons of mean energy 2.2, 3.4, 6.7, and 8.7 eV elastically scattered through angles between 20° and 60° by argon atoms are presented. Sources of experimental error are discussed and comparison with recent theoretical calculations is made.

In this Letter directly measured values of differential cross sections for the elastic scattering of positrons by gas atoms are reported. During the past decade the experimental determination of positron-atom total scattering cross sections¹⁻³ has ensued from the discovery that a small fraction (typically 10^{-5} or 10^{-6}) of fast positrons incident upon a solid surface are moderated and reemitted with a narrow spectrum of energies peaked at about 1 eV or less. The time-of-flight (TOF) technique⁴ is particularly suited to differential-cross-section measurements for positrons where, using currently available source/moderator assemblies, the scattered intensity into a detector subtending a small solid angle at the scattering center would be impractically low. Spatial separation is replaced by TOF separation, and intensities over all forward angles can, in principle, be measured simultaneously.

The TOF spectrometer designed for these measurements utilizes a source assembly similar to that described by Coleman *et al.*⁵; fast pos-

itrons from a $30\text{-}\mu\text{Ci } ^{22}\text{Na}$ source pass through a 0.25-mm-thick fast-plastic-scintillator disk, and almost all positrons emerging from the disk have produced a light flash which initiated a fast electrical timing pulse in the photomultiplier tube. The fast positrons then strike a circular 325-gauge (40% transmission) stainless steel grid coated thinly with MgO powder and the slow positrons which emerge, at a rate of about 10 sec^{-1} from the 10-mm-diam grid, possess a mean energy $\bar{E} \approx 1.6 \text{ eV}$ with a spread of about 1.5 eV. The slow positrons are accelerated axially in the 1-mm gap between the coated grid, to which a potential V is applied, and a 325-gauge grounded grid.

The diameter of the positron beam is determined by the 3.5-mm-diam hole in the brass plate which supports the grounded grid. The flux of slow positrons which passes through the hole is reduced to about 0.5 sec^{-1} . The brass plate forms the top of a 10-mm-long gas cell in which the scattering takes place. The slow positrons